Available online at www.sciencedirect.com
SCIENCE DIRECT®

Journal of the European Ceramic Society 23 (2003) 1199–1206
www.elsevier.com/locate/jeurceramsoc

Effect of spray coated SiO_2 layers on the low temperature oxidation of Si_3N_4

Sea-Hoon Lee[a,*,1], Georg Rixecker[a], Fritz Aldinger[a], Sung-Churl Choi[b], Keun-Ho Auh[b]

[a] *Max-Planck-Institut für Metallforschung and Institut für Nichtmetallische Anorganische Materialien, Universität Stuttgart, Pulvermetallurgisches Laboratorium, Heisenbergstrasse 5, 70569 Stuttgart, Germany*

[b] *Department of Ceramic Engineering, Hanyang University, #17, Haengdang-dong, Sungdong-Gu, Seoul 133-791, South Korea*

Received 14 June 2001; received in revised form 30 August 2002; accepted 7 September 2002

Abstract

Si_3N_4 using Y_2O_3 as a sintering additive provides good mechanical properties and high temperature oxidation resistance, but can suffer from crack formation when oxidized at 1000 °C. In order to minimize this problem, a SiO_2 layer was deposited onto Si_3N_4 by the spray coating method. The dispersion of the SiO_2 slurry for the spray coating process was optimized, and dense silicate layers were formed by the spray coating and heat treatment in nitrogen atmosphere. Penetration of the coating layer into the sample was observed when the heat treatment temperature was higher than 1400 °C. The crystallization behavior of silicate coatings is similar to that of native oxide layers, but the formation of cristobalite is suppressed. The SiO_2 coating inhibits the rapid oxidation of Si_3N_4 at 1000 °C effectively.

Keywords: Coatings; Oxidation; Si_3N_4; SiO_2; Spray coating

---

1. Introduction

Y_2O_3-based liquid-phase sintered Si_3N_4 is one of the most intensively investigated structural ceramics due to its excellent mechanical and thermal properties. However, its application is effectively limited due to the catastrophic failure caused by the volume expansion of secondary phases, like $Y_2Si_3O_3N_4$, during oxidation at intermediate temperature (~1000 °C). A Hooke's law estimation[1] shows that a total volume expansion of 1% generates a stress of about 1 GPa, which is of the same order of magnitude as the fracture strength of a fully dense silicon nitride ceramic. By adding Al_2O_3 [2] or SiO_2,[3] the oxidation can be decreased substantially, but mechanical properties and oxidation resistance in the passive oxidation region (> 1200 °C) are degraded. Using rare-earth oxides as sintering additives has been reported as a way to prevent this problem.[4] When rare earth oxides are introduced into a Si_3N_4, however, the high refractoriness of the grain boundary phases causes an insufficient sintering behavior, and normally hot pressing or gas pressure sintering is used to get a dense sample.

Flash oxidation has been proven to be another satisfactory solution to the problem.[5] This method consists of pre-oxidizing the specimens at a temperature above the catastrophic region so that the surface of Si_3N_4 is covered with a silica-based protective layer. Disadvantages of this technique are pit or flaw formation during the oxidation, which can decrease the mechanical properties of the material. An alternative technique is protective SiO_2 surface layers deposited by spray coating. Spray coating is used in classical ceramics to glaze porcelain. It has several advantages, like ease of processing and low production costs. F. Buchanan et al.[6] used a spray coating technique to form a oxidation protective layer onto carbon–carbon composites. They mixed isopropyl alcohol, an oil-based binder, and powder of boro-silicate glass to form a slurry which was sprayed onto the composite. During heat treatment, the sprayed layer formed a dense boro-silicate coating.

In the present experiment, the dispersion of a SiO_2 slurry was optimized for the spray coating process. The microstructure and crystallization behavior of the sili-

---

* Corresponding author.
E-mail address: lee@aldix.mpi-stuttgart.mpg.de (S.-H. Lee).

[1] Delegated to MPI für Metallforschung by Hanyang University.

0955-2219/03/$ - see front matter © 2002 Elsevier Science Ltd. All rights reserved.
PII: S0955-2219(02)00295-9

cate layers formed by the coating method were observed and compared to those formed by the oxidation of Si_3N_4. Finally, the oxidation behavior of Si_3N_4 at 1000 °C, with and without protective silicate layers, was investigated.

2. Experimental

2.1. Sintering of Si_3N_4

Table 1 shows the compositions of the materials studied. Sys 1 suffers from the 1000 °C oxidation problem. Sys 2 is one of the most common compositions of commercial products. Sys 3 and Sys 4 are spray-coated versions of Sys 1 and Sys 2, respectively. The starting powders were dried in a vacuum oven at 250 °C for 24 h, and were mixed for 4 h by planetary milling with isopropyl alcohol, followed by 24 h in a tumbling mixer. Si_3N_4 balls were used for the milling process. The powder mixtures were dried at 70 °C for 24 h using a magnetic stirrer and were compacted at 600 MPa using a cold isostatic press into 4×4×4 mm. The powder compacts were embedded in powder beds,[7] and were sintered in 0.22 MPa N_2 at 1700 °C for 3 h.

2.2. Optimization of SiO_2 slurry and spray coating

A proper viscosity of the glaze is important to get a homogeneous coating layer by the spray coating method. If the viscosity of the glaze is too high, the sprayed droplet size tends to increase,[8] and inhomogeneous coating layers are obtained. An organic binder [PVA (polyvinyl alcohol)] is used to increase the adhesion and strength of the sprayed layer.[9] In order to optimize the dispersion conditions, the iso-electric point (IEP) of aqueous SiO_2 slurries was measured using a zeta potential probe (Zetamaster, Malvern). A 20 wt.% SiO_2 slurry (purity $>$ 99.5%, average particle size : 2.16 μm) was first fabricated using a planetary mill for 5 h. The slurry was diluted with double distilled water using a magnetic stirrer for 2 h. The pH value of the diluted slurry was controlled using HCl and NH_3 solutions, and then the slurry was stirred for 2 h before the zeta potential measurement. A 20 wt.% SiO_2 slurry with 0.5 wt.% PVA was sprayed onto the surfaces of the samples using an air brush (EP-17, ECC). The spray coated samples were dried in air for 24 h and then in a oven at 50 °C for 24 h. With the increase of the film thickness, the size of cristobalite formed in the coating during the heat treatment also increases. The β to α transition of cristobalite during cooling is reported as the main reason of crack formation in the silicate layer.[10] Accordingly, thin SiO_2 coatings (<5 μm) were fabricated to minimize the crack formation during the repeated heat treatment.

2.3. Heat treatment of the coating layer and oxidation measurement

The binder in the spray-coated layer was removed in air by the heating schedule shown in Fig. 1 (a). Some cracks were observed in sprayed layers annealed with higher heating rates, which can be due to the fast thermal decomposition of PVA. After removing the binder, the samples were heat treated in 0.22 MPa N_2 atmosphere at temperatures between 1300 and 1500 °C to form a dense layer on Si_3N_4 [Fig. 1(b)].

Flash oxidized samples are reported to suffer from the 1000 °C oxidation problem if the protective silicate layer is damaged.[1] To investigate the effect of surface damage on the oxidation at 1000 °C, the coating layers were etched with diluted HF solution (8%), and the weight gain behavior of samples prepared by different methods (Sys 1, Sys 2, Sys 3, etched Sys 3, Sys 4, and etched Sys 4) was investigated. The silicate layer remains after 20 min of etching, but most of it is removed after 40 min. An over-etched microstructure is observed when the etching time is longer than 40 minutes. Therefore, the etching time of the silicate layer was fixed at 40 min.

Prior to the oxidation studies, the samples were cleaned in sequence with de-ionized water, isopropyl alcohol and acetone.[11] The cleaned samples were put on a platinum plate, and the plate was placed in an alumina boat with alumina cap.[12] The samples were heated in air at 1000 °C up to 650 h, and the weight gain of the samples by oxidation was measured. For the quantitative analysis of oxidation behavior, weight gain should be expressed by gm^{-2}. The surface of the samples in the experiment, however, had thin (~several μm) coatings and accordingly the samples were not polished.

Table 1
Compositions of the materials

System	Si_3N_4 (wt.%)	Y_2O_3 (wt.%)	Al_2O_3 (wt.%)	MgO (wt.%)	SiO_2 (coating)
Powder designation	UBE SN E10	H. C. Starck grade C	Teimei chem. ultra pure	Merck extra pure	Cerac Inc. S-1061
Sys 1	88	10	–	2	No
Sys 2	91	6	3	–	No
Sys 3	88	10	–	2	Yes
Sys 4	91	6	3	–	Yes

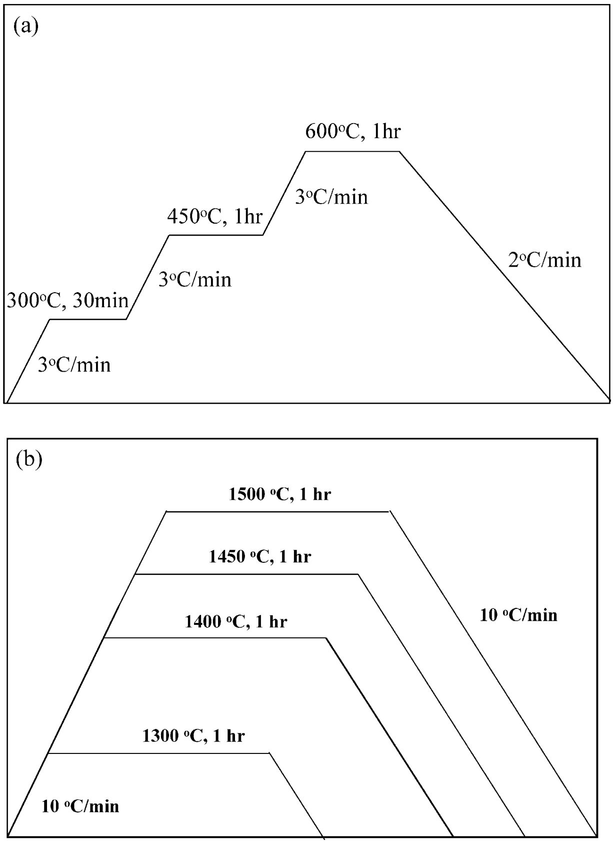

Fig. 1. Heat treatment conditions: (a) removal of binder (b) melting of SiO_2 coating.

The microstructures and compositions of the samples were observed by scanning electron microscopy (Stereoscan 200, Oxford), energy dispersive spectroscopy (Pentafet, Oxford) and X-ray powder diffractometry (D 5000, Siemens).

3. Results and discussion

3.1. Sintering of Si_3N_4

The weight loss and shrinkage of Sys 1 and Sys 2 during sintering and the density of the sintered sample are shown in Table 2. Both the samples show low weight losses and high sintering shrinkage. $Y_2Si_3O_3N_4$ and $MgSiO_3$ were formed in Sys 1 (Fig. 4), and $Y_{10}Si_3Al_2O_{18}N_4$ was formed in Sys 2 as second phases (Fig. 7).

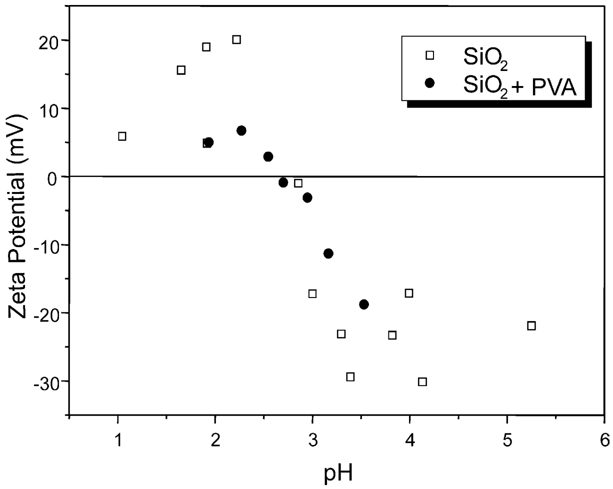

Fig. 2. Zeta potential of SiO_2 slurries with and without 0.5 w/o PVA.

3.2. Fabrication of the SiO_2 slurry for spray coating

The rheological behavior of aqueous slurries can be controlled by changing the pH of the system.[13] The particles in the slurry loose their repulsive electrostatic interaction as the pH of the system approaches to the iso-electric point (IEP). As a result, agglomeration of the particles occurs and the viscosity of the slurry increases. The IEP of quartz is known to be pH 2–2.2.[14,15] The IEP value of quartz changes with processing condition due to the different degree of hydration of their surfaces.[16] The surface of silica is covered by silanol groups, whereas the surface of quartz is relatively inert, being covered mostly by siloxane groups. The number of these groups can be changed by ball milling, which affects the IEP of the SiO_2 slurry. Fig. 2 shows the zeta potential values of the SiO_2 slurry versus pH. The IEP of the slurry is at pH 2.8. The absolute value of the zeta potential is decreased by adding PVA, but the IEP is not much affected by the addition of that binder.[17] The zeta potential value changes through the region of pH 2.5–4. Therefore, the slurry was adjusted to pH 5 for the spray coating. The relative density of the coating before the heat treatment could not be measured, because it was very weak. It tended to break into powder during mercury porosimetry measurement. After the heat treatment, the sprayed coating formed a dense layer.

Table 2
Sintering properties of Sys 1 and Sys 2

	Weight loss after sintering (%)	Sintering shrinkage (%)	Relative density (%)
Sys 1	0.12	18.12	94.5
Sys 2	1.32	17.93	95.8

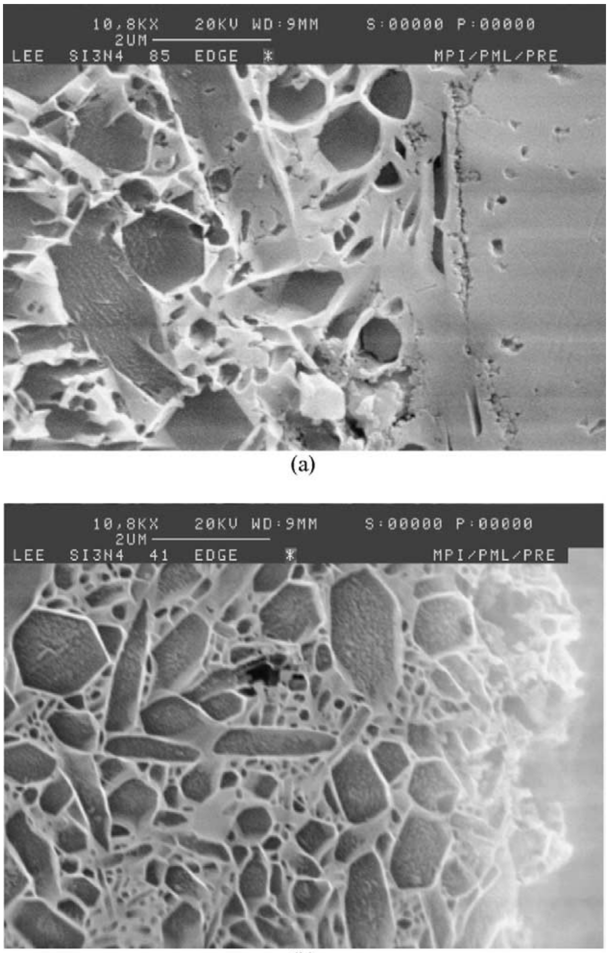

(a)

(b)

Fig. 3. Microstructure of Sys 3 vs. heat treatment conditions: (a) 1400 °C (b) 1500 °C.

Table 3
EDS analysis of SiO_2-coated and heat treated sample at different region in Fig. 5(c) (at.%)

Element	Region		
	A	B	C
Y	5.23	5.64	5.59
Al	2.77	1.61	1.71
O	2.58	1.66	1.81

3.3. *Heat treatment of the coating and microstructure examination*

The silicate layer which was heat treated at 1300 °C peeled off from the substrate, while a dense layer was formed when the heat treatment temperature was at 1400 °C. The lowest ternary eutectic point of the SiO_2–MgO–Y_2O_3 system is 1385 °C,[18] and the heat treatment temperature of Sys 3 should be higher than 1385 °C to form a liquid phase on the surface of Si_3N_4.

During the heat treatment of spray coated samples in N_2 at 1400 °C, the pore formation is suppressed, because oxygen, which causes the pore formation by the reaction $2Si_3N_{4(s)} + 3O_{2(g)} \rightarrow 6SiO_{(g)} + 4N_{2(g)}$, can not be supplied.

It has been observed using TEM that the oxide scale on the surface of Si_3N_4 penetrates between the Si_3N_4 grains during oxidation.[19] A widening of the intergranular spacing below the oxide scale has also been reported.[20] Fig. 3 shows the microstructure of Sys 3 depending on the heat treatment conditions. A silicate layer of average thickness 3 μm is formed on the surface of Si_3N_4 when the heat treatment temperature is 1400 °C [Fig. 3(a)], while little silicate layer survives on the surface of Si_3N_4 when the heat treatment temperature is 1500 °C [Fig. 3(b)]. In Sys 3, $Y_2Si_2O_7$ is formed after heat treatment in N_2 at 1400 °C, but no cristobalite reflections could be detected (Fig. 4). The $Y_2Si_2O_7$ disappears when the heat treatment temperature of Sys 3 is 1500 °C, thus the XRD pattern of Sys 3 becomes similar to that of Sys 1. Babini et al. report[21] on the phase formation of Si_3N_4 during oxidation using MgO and Y_2O_3 as sintering additives. In their report, the amount of $Y_2Si_2O_7$ increases rapidly at 1385 °C. Over 1400 °C, $Y_2Si_2O_7$ peaks decrease, and cristobalite is stated to be the main phase up to 1500 °C.

Fig. 5 shows the morphology of samples of Sys 2 and Sys 4 with different heat treatment conditions. The dark inner region of samples of Sys 4 recedes with increasing heat treatment temperature, which can be explained by the penetration of silicate layer into the samples, together with the diffusion of metal ions. Table 3 shows the oxygen, Al and Y content of sample in Fig. 5(c). The oxygen and Al content in region A is higher than that of inner region.

Table 4
The weight gains (%) of samples after oxidation at 1000 °C

System		Sys 1	Sys 3	Sys 3(etched)	Sys 2	Sys 4	Sys 4 (etched)
Weight gain (%)	24 h	0.20	0	0	0	0	0
	72 h	0.41	0	0	0.12	0.05	0.12
	144 h	0.43	0	0	0.14	0.05	0.15
	350 h	0.47	0.04	0	0.14	0.05	0.15
	650 h	0.50	0.04	0	0.19	0.08	0.15

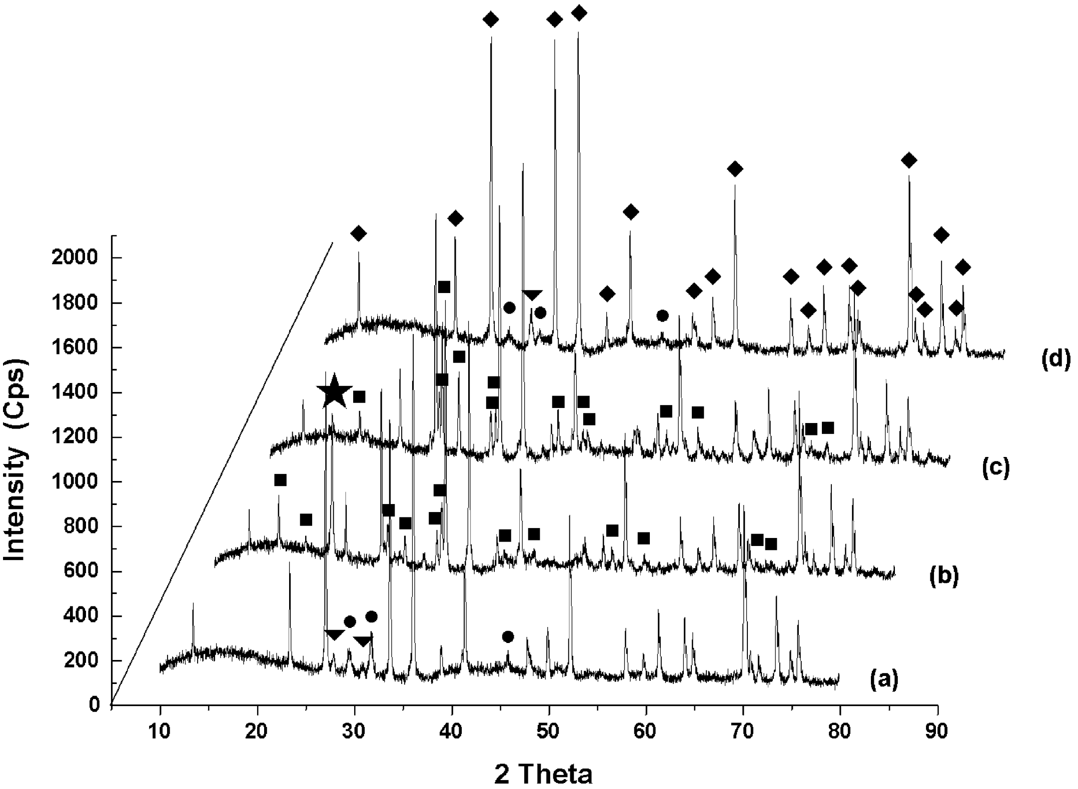

Fig. 4. XRD data after the heat treatment (a) Sys 1, after sintering (b) Sys 1, after oxidation at 1400 °C (c) Sys 3, after heat treatment in N_2 at 1400 °C (d) Sys 3, after heat treatment in N_2 at 1500 °C [◆ : β-Si_3N_4, ■ : $Y_2Si_2O_7$, ● : $Y_2Si_3O_3N_4$, ▼ : $MgSiO_3$, ★ : SiO_2 (cristobalite)].

A silicate layer with 2 μm thickness is formed after the heat treatment of Sys 4 at 1400 °C [Fig. 6(a)], but the layer vanishes with increasing the heat treatment temperature. The lowest eutectic temperature of the SiO_2–Al_2O_3–Y_2O_3 system is 1371 °C.[22] Part of the silicate layer survives after the heat treatment at 1450 °C [Fig. 6(b)], and the penetration of the silicate phase can be clearly seen below the surface of the sample. The silicate layer is not observed when the heat treatment temperature is 1500 °C. The penetrated silicate is not clearly seen in Fig. 6(c), which is likely to be due to a more homogeneous distribution of the silicate phase in the samples at 1500 °C. In all cases, pore formation is not observed below the surface of Sys 4. $Y_2Si_2O_7$, together with small amounts of SiO_2 (cristobalite), are formed in Sys 4 heat treated in N_2 at 1400 °C (Fig. 7), which disappears, when the heat treatment temperature of Sys 4 is 1500 °C, and the XRD pattern becomes similar to that of Sys 2 except for the phase $Y_5Si_3O_{12}N$.[23]

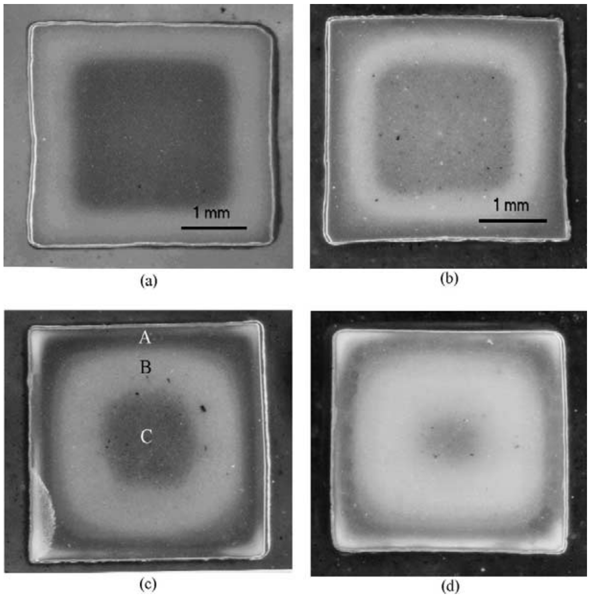

Fig. 5. Coloring of samples (cross-section) vs. heat treatment conditions (a) Sys 2 (b) Sys 4, 1400 °C (c) Sys 4, 1450 °C (d) Sys 4, 1500 °C.

3.4. Oxidation behavior

Table 4 shows the weight gain of samples after oxidation at 1000 °C. When Al_2O_3 was used as a sintering additive together with Y_2O_3 (Sys 2, Sys 4), the weight gain by oxidation is not strongly affected by the surface treatment. The weight gain decreased by the silicate layer in Sys 4, while the effect faded away after etching. In contrast, spray coating technique do affect the 1000 °C oxidation behaviors of Sys 1 and Sys 3 even after removing the protective layer. The microstructure

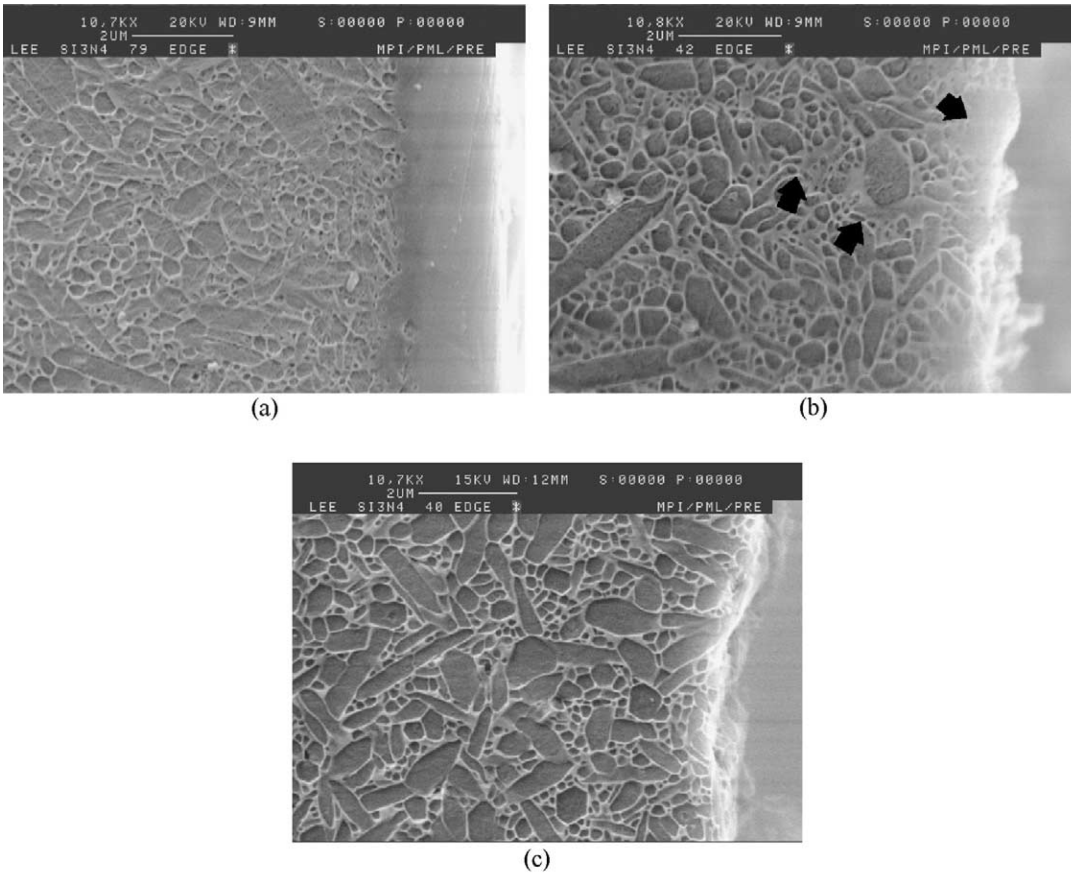

Fig. 6. Microstructure of Sys 4 with heat treatment conditions (a) 1400 °C (b) 1450 °C (c) 1500 °C (→ : silicate phase from the coating layer).

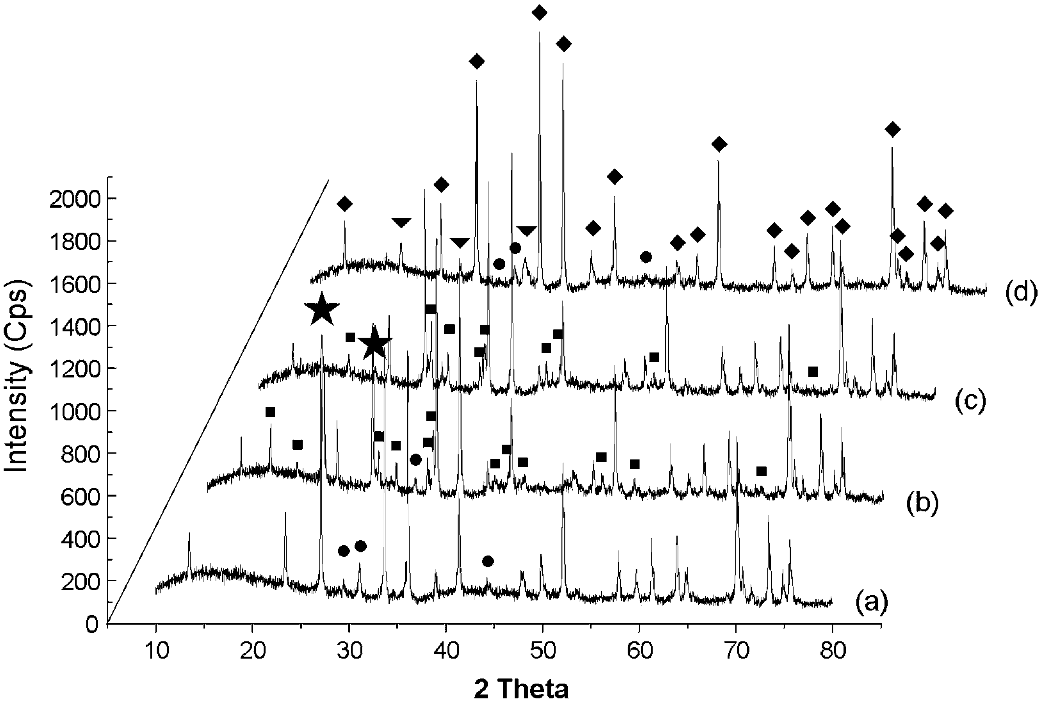

Fig. 7. XRD data after the heat treatment (a) Sys 2, after sintering (b) Sys 2, after oxidation at 1400 °C (c) Sys 4, after heat treatment in N_2 at 1400 °C (d) Sys 4, after heat treatment in N_2 at 1500 °C [◆ : β-Si_3N_4, ● : $Y_{10}Si_3Al_2O_{18}N_4$, ■ : $Y_2Si_2O_7$, ▼ : $Y_5Si_3O_{12}N$, ★ : SiO_2 (cristobalite)].

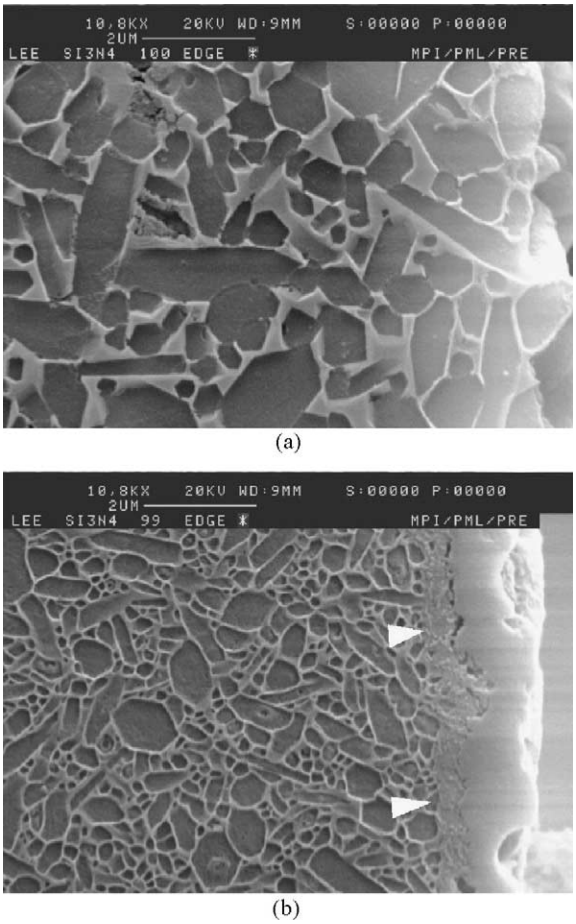

Fig. 8. Microstructure of samples after 72 h of oxidation at 1000 °C : (a) flash oxidized and etched (40 min) Sys 1 (b) Sys 4 etched for 20 min (▷ : silicate phase formed by oxidation under the residual coating layer).

of oxidized samples (Fig. 8) gives a hint to understand the different weight gain behavior. A silicate layer is not formed on the surface of flash oxidized and etched Sys 1 after 72 h of oxidation even if the weight of the sample increases by 0.22%. Looking at Sys 4, a new silicate layer is formed under the coating layer, which can clearly explain the 0.12% weight gain. The results suggest that the weight gain of Sys 1 originates from the oxidation of the $Y_2Si_2O_3N_4$ phase which is located in the grain boundary, while the oxidation of Sys 2 and Sys 4 follows the ordinary passive oxidation mechanism of Si_3N_4.

The oxidation of Sys 2 and Sys 4 is very slow at 1000 °C, but the protective silicate layer suppressed the weight gain into half even after 650 h. The benefit of the protective coating is more significant in case of the secondary phase oxidation problem at 1000 °C. The weight gain of Sys 1 is 12 times more than that of Sys 3. Since SiO_2 and Si_3N_4 phases are very stable at this temperature, a prolonged protective effect is expected by the spray coated layer.

4. Conclusions

From the results outlined above, the following conclusions can be drawn :

- Dense silicate layers on Si_3N_4 are obtained by the cost-effective spray coating method.
- $Y_2Si_2O_7$ is formed in the coated silicate layer after the heat treatment at 1400 °C, while cristobalite formation, which happens in the silicate layer formed by oxidation, is suppressed.
- $Y_2Si_2O_7$ and the silicate coating layer disappear after a heat treatment in N_2 at 1500 °C, which is likely to be due to the penetration of silicate melt into the samples.
- Spray coating decreases the oxidation rate of $Y_2Si_2O_3N_4$ phase at 1000 °C for a prolonged time, and the protective effect of which is maintained even after etching the protective silicate layer with HF.

Acknowledgements

The support of this research work by the Korea Science and Engineering Foundation (KOSEF) is greatly appreciated.

References

1. Patel, J. K. and Thompson, P. D., The low temperature oxidation problem in yttria-densified silicon nitride ceramics. *Br. Ceram. Trans. J.*, 1988, **87**, 70–73.
2. Costa Oliviera, F. A., Fordham, R. J., Canetoli, S. and de Wit, J. H. W., In-situ observation of the oxidation behavior of a silicon nitride densified with the aid of Y_2O_3 and Al_2O_3 by hot-stage microscopy. *Key Eng. Mater.*, 1996, **113**, 91–98.
3. Jack, K. H., The relationship of phase diagrams to research and development of Sialon. In *Phase Diagrams,* Vol. 5, ed. A. M. Alper. Academic Press, 1978, pp. 241–285.
4. Mieskowski, D. M. and Sanders, W. A., Oxidation of silicon nitride sintered with rare-earth oxide additions. *J. Am. Ceram. Soc.*, 1985, **68**(7), C160–C163.
5. Ritter, Jr., J. E., Jakus, K., Strazdis, L. A. and Rogers, W. P., Effect of high-temperature exposure in air on strength of hot-pressed silicon nitride. *J. Am. Ceram. Soc., 1983, C54.*
6. Buchanan, F. J. and Little, J. A., Oxidation protection of carbon-carbon composites using chemical vapour deposition and glaze technology. *Corr. Sci.*, 1993, **35**(5–8), 1243–1250.
7. Lee, S.-H., Rixecker, G., Aldinger, F., Choi, S.-C. and Auh, K.-H., Effects of powder bed conditions on the liquid-phase sintering of Si_3N_4. *J. Mater. Res.*, 2002, **17**(2), 465–472.
8. Masters, K., *Spray Drying Handbook*. Longman Scientific & Technical, 1985, pp. 244–245.
9. Hyndmann, C. P. and Tomlinson, W. J., Protective coating on RBSN. *Ceram. Int.*, 1999, **25**, 293–295.
10. Mukundhan, P., Wu, J. and Du, H. H., Oxidation behavior of NBD 200 silicon nitride ceramics. *J. Am. Ceram. Soc.*, 1999, **82**(8), 2260–2262.

11. Cinibulk, M. K. and Thomas, G., Oxidation behavior of rare-earth disilicate-silicon nitride ceramics. *J. Am. Ceram. Soc.*, 1992, **75**(8), 2044–2049.
12. Maeda, M., Nakamura, K. and Tsuge, A., Scale effect of the testing furnace on the oxidation of silicon nitride ceramics. *J. Mater. Sci. Lett.*, 1989, **8**, 195–197.
13. Reed, J. S., *Introduction to the Principles of Ceramic Processing*. John Wiley & Sons, 1988, pp. 244–247.
14. Meyer, R. J., *Gmelins Handbuch der Anorganischen Chemie*. Silicium Teil B, 1959, pp. 403–404.
15. Parks, G. A., The isoelectric points of solid oxides, solid hydroxides, and aqueous hydroxo complex systems. *Chem. Rev.*, 1965, **65**, 177–198.
16. Know, D., The stability of silica and quartz suspensions. *J. Coll. Inter. Sci.*, 1976, **54**(3), 460–462.
17. Kim, B. H., Kim, M. H., Lee, S. and Paik, U., Polymeric interactions of dispersants and binder in aqueous silicon nitride suspensions. *J. Kor. Ceram. Soc.*, 1995, **32**(8), 901–908.
18. Andrews, P. and Riley, F. L., The microstructure and composition of oxide films formed during high temperature oxidation of a sintered silicon nitride. *J. Eur. Ceram. Soc.*, 1989, **5**, 245–256.
19. Backhaus-Ricoult, M. and Gogotsi, Y. G., Identification of oxidation mechanisms in silicon nitride ceramics by TEM. *Key Eng. Mater.*, 1996, **113**, 81–90.
20. O'meare, C. and Sjöberg, J., Transmission electron microscopy investigation of the oxidation of hot isostatically pressed silicon nitride with and without sintering aids. *J. Am. Ceram. Soc.*, 1997, **80**(6), 1491–1500.
21. Babini, G. C., Bellosi, A. and Vincenzini, P., Oxidation of silicon nitride hot pressed with $Y_2O_3 + MgO$. *J. Mater. Sci.*, 1983, **18**, 231–244.
22. Kolitsch, U., Seifert, H. J., Ludwig, T. and Aldinger, F., Phase equilibria and crystal chemistry in the Y_2O_3-Al_2O_3-SiO_2 system. *J. Mater. Res.*, 1999, **14**, 447–455.
23. Wang, L., He, C. and Wu, J., Oxidation of sintered silicon nitride: 1. Phase composition and microstructure. *Mater. Sci. Eng.*, 1992, **A157**, 125–130.